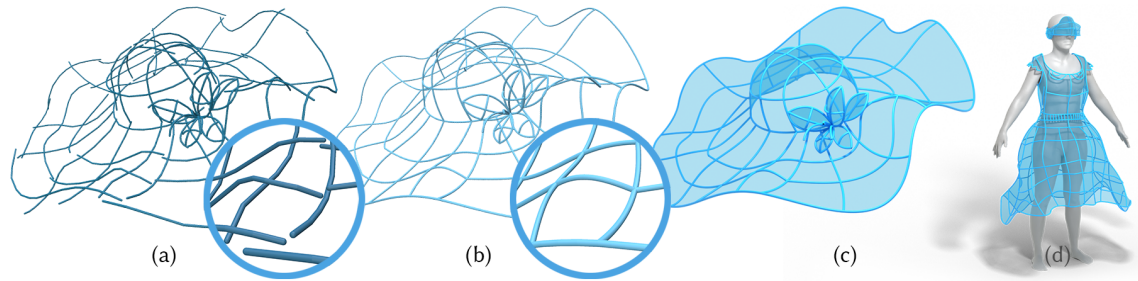


1 CASSIE: Curve and Surface Sketching in Immersive Environments

2 ANONYMOUS AUTHOR(S)

3 SUBMISSION ID: 6465



18 Fig. 1. Freehand 3D sketching in AR/VR allows rapid conceptualization of design ideas (a). However, 3D inputs are prone to large
19 inaccuracies (a, inset) and sketches cannot be utilized in downstream design pipelines. Our novel 3D sketching system, CASSIE,
20 allows the creation of clean, well-connected 3D curve networks by performing automatic stroke neatening (b). These curve networks
21 are augmented by our on-the-fly cycle detection and surfacing method (c) which improves shape perception by providing occlusion
22 cues. We evaluated CASSIE with 12 users and utilized it for creating 3D concepts for a variety of application domains (d).

23 We present CASSIE, a conceptual modeling system in VR that leverages freehand mid-air sketching, and a novel 3D optimization
24 framework to create connected curve network *armatures*, predictively surfaced using *patches* with C^0 continuity. Our system provides
25 a judicious balance of interactivity and automation, providing a homogeneous 3D drawing interface for a mix of freehand curves,
26 curve networks, and surface patches. Our system encourages and aids users in drawing consistent networks of curves, easing the
27 transition from freehand ideation to concept modeling. A comprehensive user study with professional designers as well as amateurs
28 ($N=12$), and a diverse gallery of 3D models, show our armature and patch functionality to offer a user experience and expressivity on
29 par with freehand ideation, while creating sophisticated concept models for downstream applications.

30 CCS Concepts: • Computing methodologies → Virtual reality; Shape modeling.

31 Additional Key Words and Phrases: curve networks, beautification, immersive design

32 ACM Reference Format:

33 Anonymous Author(s). 2021. CASSIE: Curve and Surface Sketching in Immersive Environments. In *Proceedings of CHI '21: ACM CHI
34 Conference on Human Factors in Computing Systems (CHI '21)*. ACM, New York, NY, USA, 20 pages. <https://doi.org/10.1145/x.xxx>

35 1 INTRODUCTION

36 The digital 3D realization of a mental design construct typically progresses from exploratory *ideation* to a *concept model*
37 which is subsequently processed for presentation, structural analysis, or manufacturing [16, 41]. Freehand sketching,
38 traditionally on pen and paper, dominates the ideation process. A number of digital 2D drawing interfaces support the

39 Permission to make digital or hard copies of all or part of this work for personal or classroom use is granted without fee provided that copies are not
40 made or distributed for profit or commercial advantage and that copies bear this notice and the full citation on the first page. Copyrights for components
41 of this work owned by others than ACM must be honored. Abstracting with credit is permitted. To copy otherwise, or republish, to post on servers or to
42 redistribute to lists, requires prior specific permission and/or a fee. Request permissions from permissions@acm.org.

43 © 2021 Association for Computing Machinery.

44 Manuscript submitted to ACM

105 creation [7, 15, 38] and exploration [2] of ideation sketches. These sketches serve as a visual reference for concept 3D
106 CAD modeling [6], though recent works like Analytic Scaffolding [47] and True2Form [55] have shown that 2D design
107 sketches can be lifted into 3D curve networks, effectively bridging 2D interfaces for ideation and concept modeling.
108

109 In the immersive environments of Augmented and Virtual Realities (AR/VR), a sketch-pen becomes a magic wand,
110 allowing users to step into their creations and draw directly in 3D. Popular VR applications like Tilt Brush [21] and
111 Quill [18], that facilitate direct 3D creation and viewing of designs at diverse scales (even in-situ for AR [3]), suggest
112 that sketching in immersive environments has the potential to completely disrupt 3D ideation. Analogous to True2Form
113 [55], our system *CASSIE*, shows that 3D *freehand* sketching optimized to create curve network *armatures*, surfaced by
114 predictive *patches*, can bridge ideation and concept modeling in VR.
115

116 Existing research and commercial software for 3D modeling in VR is based on disparate metaphors of free-form
117 sculpting [18], CAD-like curve and surface creation [24], curve networks [54], swept surfaces [13], hybrid 2D/3D model
118 creation [3], and even coarse-to-fine poly modeling [22]. In contrast, CASSIE is the first general ideation and concept
119 modeling system that progressively transforms mid-air sketch strokes into patched 3D curve networks. Admittedly, the
120 distinction between 3D ideation and concept models becomes subtle in VR when both are produced via a sketching tool
121 such as CASSIE. In the subsequent text, we will use the following definitions:
122

- 123
- 124 – An *ideation* sketch serves as an externalization of a mentally evolving design. In our system such sketches consist of
125 independent strokes from which a surface cannot trivially be inferred.
126
 - 127 – A *concept model* expresses the design as a well-defined shape that designers use to communicate their idea to others.
128 It loses part of the ambiguity present in ideation, thereby gaining structure which enables refinement and reuse. In
129 our system, concept models consist of connected curves which form a network that aids us in computing meaningful
130 surface patches.
131

132

133 Inspired by interactive sketch beautification [20, 30], we automaticallyneaten strokes as they are drawn to detect and
134 enforce intersections with nearby curves and 3D grid points, tangent continuity, axis-alignment, and planarity—features
135 that are common in man-made objects [55]. Uniformly applying multiple and potentially conflicting sketch constraints
136 can cause neated strokes to deviate from their design intent. We thus cast the selection of these criteria as selective
137 3D optimization, balancing geometric constraint satisfaction with fidelity to the sketched stroke. We further propose a
138 real-time algorithm, inspired by Stanko et al. [50], to progressively construct surface patches across predicted cycles
139 of network curves. The resulting surfaces serve a triple purpose: they incrementally bolster the 3D shape providing
140 important depth and occlusion cues [5]; they serve as virtual canvases on which to draw or project additional detail
141 curves; and they act as an ongoing incentive to draw consistent curve networks, naturally guiding the user from
142 ambiguous ideation curves towards a well-defined 3D concept model.
143

144 While CASSIE embodies functionality to support both 3D ideation and conceptual modeling, we formally evaluate its
145 salient features as three independent systems: *freehand* mid-air drawing with minimal and independent smoothing of
146 3D user strokes; *armature*, which enables overall stroke optimization to aid the creation of precise curve networks; and
147 *patch* which further enables the automatic detection and surfacing of appropriate curve network cycles. We conducted
148 a within-subjects study of the 3 systems with 12 users (design professionals or enthusiasts). The study validated the
149 functional need for all aspects of CASSIE: *freehand* sketching for ideation, and *armature* and *patch* for concept modeling.
150 Critically, the study showed that the complexity and constraints of our concept modeling functionality were achieved
151 with an agency and overall user experience comparable to unconstrained ideation sketching. While our study data
152

153
154
155
156
157
158
159
160
161
162
163
164
165
166
167
168
169
170
171
172
173
174
175
176
177
178
179
180
181
182
183
184
185
186
187
188
189
190
191
192
193
194
195
196
197
198
199
200
201
202
203
204
205
206
207
208

209 shows strong support for freehand ideative exploration (Fig. 9), it equally validates our hypothesis that intermingled
210 curve network and surface creation is valuable and encourages the creation of consistent 3D conceptual models.
211

212 Some of our professional study participants were keen to continue experimenting with CASSIE after the study,
213 and we show a gallery of compelling and diverse 3D concept models created by a variety of users (Fig. 11). We also
214 demonstrate the suitability of these models for downstream sculpting, engineering, and fabrication applications (Fig. 13).
215

216 Our **contributions** are thus threefold: we present a homogeneous ideation and concept modeling system for design
217 sketching in VR, based on a novel 3D curve and surface optimization framework; we report on a detailed comparative
218 evaluation between ideation and conceptual modeling in VR, with 12 users; we provide a corpus of 3D stroke data for
219 future design analysis and data-driven mid-air sketch processing.
220

221 2 RELATED WORK

222

223 We start by discussing related work on immersive sketching, before discussing methods for sketch beautification,
224 sketch-based modeling, and surfacing of curve networks.
225

226

227 *Immersive sketching.* While our system targets modern head-mounted displays, it relates to early efforts on supporting
228 3D drawing and painting with a variety of virtual reality devices. The seminal HoloSketch allows the creation of 3D
229 shapes with geometric primitives and sweep surfaces [13]. Observing that it can be challenging to position and scale 3D
230 primitives accurately, the author included an option to snap them to a 3D grid, a solution that we also adopt. Surface
231 Drawing [46] offers similar modeling capabilities by sweeping a strip of surface along the trajectory of the user's hand.
232 Users of this system created 3D paintings by covering the intended surface with dense surface strips. A similar practice
233 is often observed with modern systems like Tilt Brush [21], where users accumulate a large number of strokes to paint
234 surfaces in VR. In contrast, we target the creation of lightweight sketches composed of a sparse network of curves,
235 which convey 3D surfaces with an economy of means. These networks, along with their surfaced patches, can be
236 readily exported to downstream 3D software rather than requiring dedicated post-processing as is the case for dense
237 3D paintings [43].
238

239 Sketching in VR brings new challenges, compared to traditional 2D sketching. Arora et al. [5] and Machuca et al.
240 [37] observed poor mid-air sketching accuracy even when users sketched simple strokes such as straight lines and
241 circles. While the former studied drawing such strokes in isolation, the latter evaluated precision and aesthetic quality
242 of shapes made of grid-aligned lines and circles. Compared to sketching on paper, the lack of a supporting surface and
243 the additional degrees of freedom induce the need for finer motor control to properly position strokes in 3D space. The
244 lack of depth cues in sparse sketches also contributes to the approximate positioning of strokes relative to each other [5].
245 This imprecision can be extremely frustrating, especially for artists transitioning from 2D sketching to AR/VR [27]. We
246 address these challenges by automatically correcting imprecise strokes and by visualizing surfaces in-between strokes.
247

248 Our work is closer in spirit to FreeDrawer [54], where users first sketch a sparse network of feature curves, and then
249 manually indicate curve cycles to form surface patches. Spacedesign [19] implements a similar concept but sketching is
250 constrained to 2D curves projected onto virtual or physical planes. While we share the design philosophy of FreeDrawer
251 and Spacedesign, we present a novel 3D optimization framework for curve network creation, as well as an algorithm for
252 progressive, automatic surface patch creation, on current VR hardware. More importantly, we report on a comprehensive
253 user study with design professionals and amateurs to evaluate the impact of these curve network and surface features,
254 for ideation and concept modeling in AR/VR.
255

313 Several other solutions have been proposed to overcome the challenges of VR sketching. The 3-Draw system [44] 365
 314 decouples the act of drawing the curve from the act of positioning it with respect to other curves. Keefe et al. [33] use 366
 315 haptic feedback from a Phantom device and a two-hand interaction metaphor inspired by tape drawing [8] to separate 367
 316 drawing the curve from indicating its tangent directions. Other two-handed systems simulate deformable rods that 368
 317 users bend to model shape outlines and sharp surface features [53], or rely on a physical strip of sensors that provides 369
 318 bending and twisting controls on 3D curves [25]. Other methods avoid or limit the use of 3D freehand sketching in 370
 319 the creation process. Jackson and Keefe [31] use curves from a 2D sketch as a basis for VR creation, a feature also 371
 320 available in the commercial software GravitySketch [24] along with other curve editing operations based on control 372
 321 points. Strokes in GravitySketch however beautiful, do not form a connected curve network, and thus require dedicated 373
 322 user intervention to create surfaces (see Section 7.1 for a comparison). Arora et al. [3] rely on a 2D tablet on which 374
 323 the artist sketches precise strokes that are then mapped to a proxy 3D surface defined by a few freehand 3D strokes. 375
 324 In a similar spirit, Kim et al. [34] capture hand motion to describe 3D scaffolding surfaces on which 2D strokes are 376
 325 projected. In contrast, our system offers a direct sketching workflow where users draw free-form 3D curves with their 377
 326 dominant hand, and only use the other hand for navigation control. 378
 327

328 Finally, Machuca et al. [36] share our goal of beautifying freehand 3D strokes, which they achieve by automatically 382
 329 detecting potential geometric relationships with existing strokes. Their approach is limited however, to planar strokes 383
 330 snapped at stroke endpoints, resulting in regular shapes dominated by straight or circular strokes lying on perpendicular 384
 331 or parallel planes. Our curve networks, in contrast, are generic, supporting highly non-planar curves (Fig. 1). 385
 332

333 In summary, CASSIE is the first integrated VR system which allows for both 3D ideation and concept modeling 387
 334 through a single, fluid sketch-based interface. 388
 335

336 *2D sketch regularization and sketch-based modeling.* Our approach to 3D stroke neatening is inspired by sketch 390
 337 beautification/regularization frameworks originally developed to process 2D diagrams and drawings created with a 391
 338 computer mouse. Pavlidis and Van Wyk [40] introduced one of the first such systems, that takes a line drawing as input 392
 339 and outputs a drawing close to the input while satisfying geometric constraints. While this system was applied as a 393
 340 post-process on complete drawings, Igarashi et al. [30] proposed an interactive beautification method that treats each 394
 341 new stroke as it is sketched. This iterative approach can cope with more complex sketches and geometric relationships 395
 342 between strokes. The interactivity of the system also gives more control to the user who can choose between multiple 396
 343 possible beautified results. More recently, Fišer et al. [20] proposed an interactive method called ShipShape, that 397
 344 supports Bézier curves as input. We draw inspiration from their approach, although we focus on a small set of geometric 398
 345 constraints tailored to the most frequent sensorimotor errors we observed in 3D sketching, while they consider a larger 399
 346 variety of rules to beautify 2D drawings. In addition, while Fišer et al. [20] beautify each stroke by applying geometric 400
 347 rules in sequence, we cast stroke neatening and structuring as an energy minimization that balances the concurrent 401
 348 application of multiple geometric constraints with preservation of the input curve. This formulation is inspired by 402
 349 sketch-based modeling algorithms that seek to lift 2D strokes to 3D by enforcing geometric constraints, while making 403
 350 sure that the resulting curves re-project well on the input drawing [12, 47, 48, 55]. In particular, the interactive system 404
 351 by Schmidt et al. [47] lifts each new stroke by snapping it to the 3D curves inferred from previous strokes, which they 405
 352 achieve by balancing the satisfaction of snapping constraints with re-projection error. 406
 353

354 *Surfacing of 3D curve networks.* Surfaced curve networks form a compact and descriptive representation of 3D 412
 355 shapes [23], which has motivated the development of algorithms to automatically generate surfaces from sparse, 413
 356 designer-drawn 3D networks. A first challenge is to identify, among all closed cycles in the curve network, which cycles 414
 357

358
 359
 360
 361
 362
 363
 364

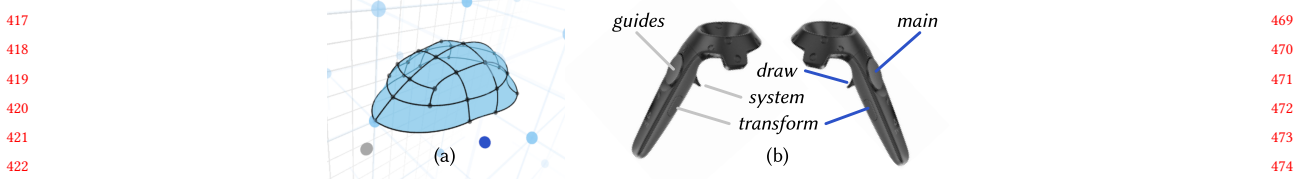


Fig. 2. Our minimal interface is designed for simplicity, allowing the user to focus on creation (a). In a similar spirit, the controls are kept minimal and easily generalize to varied hardware (b). Here we show the controls mapped to an HTC Vive controller.

bound surface patches rather than internal cross-sections. Treating this problem globally is difficult due to the large search space of all possible curve cycles in a network, and due to the inherent ambiguity of the task [1, 45, 56]. We instead leverage the iterative nature of our workflow to surface the network progressively, only performing a local search for cycles around each newly-added stroke. Our interactive context also allows us to let users add or remove cycles that might have been misinterpreted by our automatic algorithm. A second challenge is to generate the surface geometry that interpolates the cycle boundaries. We adopt the method by Zou et al. [57] for this task, which applies a dynamic programming algorithm to generate a triangulation that satisfies various geometric criteria. Alternative solutions include the generation of a quad mesh aligned with the input curves [9]. Finally, various surface fairing algorithms have been proposed to improve the quality of the generated surfaces [39, 50], and could be applied to our results in a post-process.

3 USER INTERFACE AND WORKFLOW

We first present the drawing interface offered by our system and the workflow it enables. We describe the technical components necessary to achieve this workflow—stroke neatening and surfacing—in Sections 4 and 5 respectively.

3.1 Interface elements

We endeavoured to keep the interface minimal and user interactions simple, to keep the user focused on the creative task at hand. As a secondary objective, we only assumed standard interface features, common across modern VR setups, to ease remote evaluation on a variety of consumer VR hardware.

Fig. 2a illustrates our drawing interface as seen in the VR headset. In addition to the 3D shape being created, our interface visualizes the ambient workspace with an axis-aligned 3D grid for better depth perception. The workspace also includes an optional mirror plane, which greatly facilitates the design of symmetric objects. Users interact with the system using two 6-DoF (degree of freedom) controllers, each of which must provide three push-buttons. Fig. 2b shows all the controls on the HTC Vive controller, but the interactions can be similarly mapped to other common devices.

Users can draw strokes using the *draw* button. We represent each stroke as a smooth cubic poly-Bézier curve or a straight line segment, from which we remove unintended “hooks” at extremities as done by Liu et al. [35]. Double-clicking the *main* button on the dominant-hand controller is used to delete selected curves or surface patches. Selection is implicit, based on proximity to the curve/surface. Single-clicking the *main* button is used to manually create surface patches where automatic detection fails. Holding the *transform* button on the dominant or non-dominant controller allows uniformly scaling or rigidly transforming the workspace, respectively. Clicking or double-clicking the *guides* button on the non-dominant controller toggles the grid or the mirror plane, respectively. Finally, users can completely disable the automatic curve regularization and surfacing by clicking the *system* button, and use the same button to

417
418
419
420
421
422
423
424
425
426
427
428
429
430
431
432
433
434
435
436
437
438
439
440
441
442
443
444
445
446
447
448
449
450
451
452
453
454
455
456
457
458
459
460
461
462
463
464
465
466
467
468
469
470
471
472
473
474
475
476
477
478
479
480
481
482
483
484
485
486
487
488
489
490
491
492
493
494
495
496
497
498
499
500
501
502
503
504
505
506
507
508
509
510
511
512
513
514
515
516
517
518
519
520

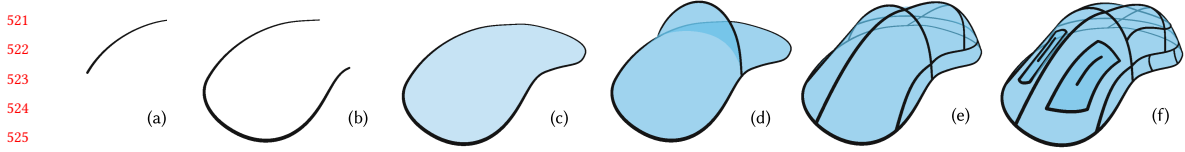


Fig. 3. Typical workflow to create a 3D concept model with CASSIE. Our system automatically connects user strokes as they are drawn to form long curves (a–c) and curve networks (d–e). We detect closed cycles in this network to form surface patches (c–e), which improves depth perception, supports the creation of surface details (f), and results in models ready for downstream applications.

toggle the predictive features on again. Note that the functionalities attributed to the *draw* and *transform* buttons are very similar to commercial VR applications [17, 21], and therefore, users can quickly grasp their function.

Visible interface elements are similarly designed to be simple and unintrusive (see Fig. 2a). Both the controllers are rendered as small spheres, differentiated by colour. The grid is rendered as semi-transparent lines and spheres. Curves are rendered in a visually-dominant black, while nodes of the curve network (intersections) are shown as faint spheres. The latter serves as an important visual confirmation of a successful connection. Patches are shown as a faint blue to provide occlusion, thus improving depth perception [5, Figure 13], without obstructing important design elements or breaking the creative flow. Finally, implicit selections are indicated by a color change.

3.2 User workflow

Fig. 3 illustrates a typical concept modeling session with our system. For every newly-drawn stroke, our system automatically identifies regularization criteria with respect to already-created 3D curves, as well as to the ambient 3D grid. In particular, the system aligns the new stroke, in position as well as tangent, to nearby curves to ease the creation of long curves (Fig. 3a–c) and well-connected curve networks (Fig. 3d–f). The system also snaps strokes to nearby grid nodes, facilitating the use of the grid as a precise scale reference.

For every new curve added to the network, our system searches for closed cycles in its vicinity to form surface patches or to modify existing ones (Fig. 3c–e). These patches greatly contribute to the perception of the 3D shape by occluding background curves. They can also serve as a sketching support, on which users can draw surface details or connect extruding parts (Fig. 3f). While the surface patches are found automatically, users can delete any patch to create holes, or add a patch where the automatic algorithm might have missed one due to ambiguity.

From the user perspective, the curve network and associated surface patches behave like a soap film, which the user shapes progressively by adding one curve at a time to form complete concept models (Fig. 3f). Note that strokes on which we detect no constraint to apply are left unchanged. Alternatively, users can also toggle all the predictive features off to fall back to a freehand sketching workflow more suitable to preliminary ideation.

4 CREATING CURVE NETWORKS

Designers often depict 3D shapes by sketching networks of curves running along surface boundaries and lines of curvature [16, 23]. These curves aid the creation of 3D meshes in downstream 3D modeling [51], and several algorithms exist to automatically surface 3D curve networks [9, 45, 56]. Unfortunately, unlike 2D sketching, 3D user strokes rarely intersect perfectly, making freehand drawing of 3D curve networks in VR difficult. We facilitate the creation of such curve networks by automatically detecting and enforcing proximal curve intersections. Complex drawings contain cluttered regions however, where enforcing all such candidate intersections for a single stroke, can distort the stroke

625 dramatically. Inspired by related work on 2D sketch beautification [20, 30] and sketch-based modeling [47, 55], we 677
 626 propose a mechanism to connect each new 3D stroke to as many nearby 3D curves as possible (discrete hard constraints) 678
 627 while staying close to its original trajectory, and compensating for drawing inaccuracy by favoring various geometric 679
 628 features including planar curves and tangent continuity (continuous soft constraints). Solving such a problem is a mix of 680
 629 a potentially exponential search for the optimal subset of discrete hard constraints to satisfy, and function minimization 681
 630 for the continuous soft constraints. 682
 631 683
 632 684
 633 685
 634 686

635 4.1 Algorithm overview 687

636 Our solution has three steps. Given a sketched 3D stroke, we first find all candidate hard intersection constraints 688
 637 using the distance between points on the stroke and existing 3D curves. We then find an approximately optimal subset 689
 638 of discrete constraints using a greedy linear search, and formulate a least squares minimization for the continuous 690
 639 constraints. Our overall algorithm is thus efficient, robust, and works well in practice without any noticeable lag. 691
 640 692
 641 We next describe our algorithm in a bottom-up fashion. We first detail our 3D curve optimization that minimizes soft 693
 642 constraints and remains as close as possible to the input stroke, while satisfying a prescribed subset of hard constraints 694
 643 (Section 4.2). We then describe our strategy to select this optimal subset (Section 4.3), and finally detail how the various 695
 644 terms of the optimization are formulated (Section 4.4). We explain how we treat the simpler case of straight lines in 696
 645 supplemental material. 697
 646 698
 647 699
 648 700
 649 701

650 4.2 Enforcing intersections via continuous optimization 702

651 Let us first assume that we have selected a set of intersections \mathcal{I} between the user stroke and existing curves in the 3D 703
 652 sketch. We associate each intersection with a constraint $c_{i \in \mathcal{I}}$ that needs to be satisfied for the user stroke to intersect 704
 653 the corresponding curve exactly. However, the input stroke needs to be deformed to satisfy these constraints. We 705
 654 measure the amount of deformation with an energy that we denote E_{fidelity} . In addition, we also seek to encourage 706
 655 regularization criteria such as curve planarity and tangential alignment to intersected curves, which we also express as 707
 656 energy terms E_{planar} and E_{tangent} . We express these criteria as soft energy terms rather than hard constraints because 708
 657 they correspond to aesthetic properties that are desirable but that can be balanced against other desiderata. In contrast, 709
 658 we need intersections to be satisfied exactly to form a well-connected curve network. Finally, we also ensure that 710
 659 the deformed stroke preserves the original G^1 continuity between successive curve segments, which we express as a 711
 660 set of constraints g_k . Given an input stroke S , we compute the deformed stroke S' that satisfies all constraints while 712
 661 minimizing deformation and best satisfying other criteria by solving the *continuous* optimization 713
 662 714
 663 715
 664 716
 665 717

$$\begin{aligned} \min_{S'} \quad & E_{\text{fidelity}}(S, S') + E_{\text{planar}}(S') + \sum_{i \in \mathcal{I}} E_{\text{tangent}}(S', i), \\ \text{s.t.} \quad & c_{i \in \mathcal{I}}(S') = 0 \\ \text{and} \quad & g_k(S') = 0. \end{aligned} \tag{1}$$

671 Recall that our strokes are represented using cubic Bézier segments. We formulate the soft constraints as quadratic 723
 672 energy functions of the Bézier control points, and hard constraints as linear functions, allowing us to solve this 724
 673 constrained least squares problem as a single linear solve as detailed in supplemental material. 725
 674 726
 675 727
 676 728

4.3 Selecting intersections via discrete optimization

New strokes often run near multiple curves, especially on complex drawings with high stroke density. Our next challenge is to identify which of these curves should intersect the input stroke. On the one hand, we would like the curve network to be as connected as possible. On the other hand, we don't want to deviate too much from the original user intent. We cast these competing objectives as two terms in a *discrete* optimization, where we model the activation of each constraint c_i with a binary variable b_i set to 1 if the intersection is selected and to 0 otherwise

$$\min_{b_i \in I} \lambda E_{\text{fidelity}}(S, S'(b)) + (1 - \lambda) E_{\text{connectivity}}(b) \quad (2)$$

where the deformed stroke $S'(b)$ is computed using Eq. (1) and the selected intersections, E_{fidelity} measures the deviation of S' from the input stroke, $E_{\text{connectivity}}$ is an energy term that decreases as more intersections are selected, and $\lambda = 0.6$ is a parameter that balances the two objectives.

Unfortunately, finding the optimal subset would require solving Eq. (1) for all $2^{|I|}$ combinations of binary variables b_i , which is impractical. Yet, we observed that the detected intersections are most often valid, and only a few superfluous ones need to be rejected. This observation motivated us to minimize Eq. (2) using a greedy strategy, where we first select all intersections, and then test all subsets obtained by removing one intersection. If the best of these subsets yields a lower energy than the full set, we keep it and repeat the process by removing another intersection, until the energy doesn't decrease anymore. Fig. 4 illustrates the result of this selection mechanism on a 2D curve, and on typical 3D curve configurations.

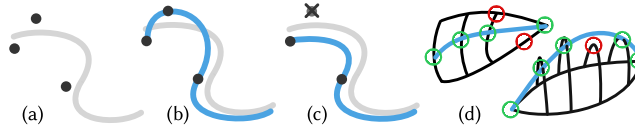


Fig. 4. An input stroke with all detected potential intersections (a). Enforcing all intersections distorts the curve (b). Enforcing the optimal subset keeps the curve close to the input (c). Typical configurations where too many intersections are detected (d): in areas with high stroke density (top) or when the input stroke is smooth but the candidate intersections do not form a smooth path (bottom). Our algorithm selects a subset of intersections (green) and rejects others (red) to preserve the shape of the original curve (blue).

4.4 Implementation details

We now describe how we detect and express the constraints and energy terms that form Eq. (1) and Eq. (2). We refer the interested reader to supplemental material for additional implementation details.

Distance and angular thresholds. Many of our regularization constraints and objectives depend on a notion of proximity between curves, in space and/or angle. In addition, we wish to make the sensitivity of our beautification process adaptive to the drawing scale, such that the beautification is less aggressive when users zoom-in to draw details. We achieve this goal by defining a spatial proximity threshold $\delta(s) = \frac{\delta^1}{s}$, where s denotes the scale of the drawing space and $\delta^1 = 4\text{cm}$ was fixed experimentally for appropriate beautification. In the initial zoomed out state, $s = 1$.

We set the angular threshold to $\theta = \frac{\pi}{6}$, under which we consider that two lines or curves are parallel.

Intersections. We detect intersections between the input stroke and any nearby curve, grid nodes or the mirror plane by testing if the brush tip comes within a radius $r_{\text{proximity}} = \delta(s)$ of such elements while sketching. We also check if the two endpoints of the stroke are within a distance $r_{\text{proximity}}$ of each other to form closed loops. We enforce an

833 intersection by inserting a control point at the closest point of the new curve and constraining it to be on the other
 834 curve or grid node.
 835

885
886
887
888
889
890
891
892
893
894
895
896
897
898
899

836 *Tangent alignment.* At each intersection, we compare the tangents between the two curves. If the angle between
 837 both tangents is under the angular threshold θ , we encourage the tangent of the new curve to align with the other one
 838 using an energy term E_{tangent} that measures the norm of their cross product. Otherwise, we set E_{tangent} to zero.
 839

891
892
893
894
895
896
897
898
899

840 *Planarity.* We first compute the best-fit plane to the control points by least squares. If the distance from the plane to
 841 the farthest control point is below the threshold $r_{\text{proximity}}$, we encourage all control points to lie in the plane using an
 842 energy E_{planar} that minimizes the dot product between the plane normal and the vectors formed by pairs of successive
 843 control points. We also test whether the plane normal is within an angle θ to one of the three orthogonal grid directions,
 844 in which case we snap the plane to be orthogonal to that direction. For non-planar curves, we set E_{planar} to zero.
 845

893
894
895
896
897
898
899

846 *Fidelity to input.* Our fidelity energy E_{fidelity} measures deviation between the beautified curve and the input one.
 847 Following Xu et al. [55], we measure both the deviation in absolute position of the control points and the deviation in
 848 the slope of pairs of successive control points, the latter term penalizing variations in the overall shape of the curve.
 849

900
901
902
903
904

850 *Connectivity.* The goal of $E_{\text{connectivity}}$ is to favor the selection of as many intersections as possible, as long as they do
 851 not overly deform the input. We model it with an exponential that increases as fewer constraints are selected
 852

905
906
907

$$E_{\text{connectivity}}(b) = e^{-\left(\frac{\sum_{i \in I} b_i w_i}{\sum_{i \in I} w_i}\right)^2}, \quad (3)$$

908
909

853 where w_i denotes the weight associated to intersection i , and b_i equals 1 if the intersection is selected, 0 otherwise.
 854 Following Schmidt et al. [47], we vary this weight depending on the nature of the intersection, being equal to 1 if
 855 the curve intersects a grid node or the mirror plane along its trajectory, 1.25 if the curve intersects a grid node at its
 856 endpoint, 1.5 if the curve intersects another curve, and 2 if the curve passes through an existing intersection.
 857

910
911
912
913
914
915

864 5 SURFACING

916
917

865 Our stroke neatening and structuring algorithm greatly facilitates the creation of well-connected curve networks, which
 866 in turn enables the automatic detection of curve cycles bounding surface patches. We first describe how we identify
 867 these cycles before detailing how we generate the surface they bound and how we exploit these surface patches for
 868 drawing on-surface details.
 869

918
919
920
921
922
923

872 5.1 Cycle detection

924
925

873 A number of existing cycle detection algorithms perform a global optimization over the complete curve network [1, 56].
 874 Unfortunately, the space of cycles of a given curve network is very large, making a global search computationally
 875 demanding and unnecessarily repetitive in an interactive system. Instead, we exploit the fact that after the user has
 876 sketched a new stroke, any new patches should only be created for cycles in parts of the network affected by the stroke.
 877 We thus apply a local search strategy, which is more suitable for real-time, incremental construction of the sketch. Our
 878 approach is inspired by the algorithm of Stanko et al. [50], which relies on the surface normal at each intersection to
 879 sort all segments incident to that intersection, such that cycles can be formed by walking around the curve network in
 880 a fixed order as illustrated in Fig. 5.
 881

926
927
928
929
930
931
932
933
934
935

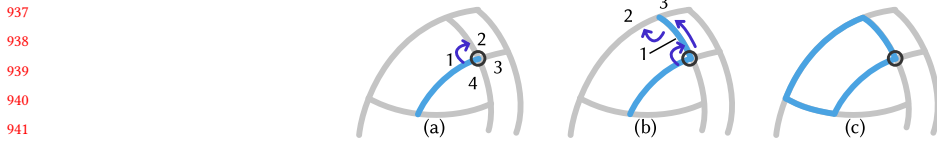


Fig. 5. Local cycle detection. We sort all segments incident to an intersection according to the surface normal at that intersection (a). We walk around the cycle by selecting at each node the next segment in clock-wise order (b), until we obtain a closed cycle (c).

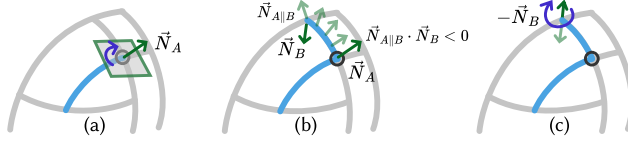


Fig. 6. Local normal orientation. We compute the surface normal \vec{N}_A at node A by fitting a plane on the tangents of incident curve segments (a). We parallel-transport this normal to node B to obtain $\vec{N}_{A||B}$, which we compare to \vec{N}_B (b). Since the two vectors point to opposite directions, we flip \vec{N}_B before proceeding (c).

However, while Stanko et al. [50] were reconstructing real-world surfaces for which the normal was measured, we need to infer the surface normal from the input curves. We obtain this normal estimate at each intersection by assuming that the intersecting curves lie on a smooth surface, whose tangent plane is spanned by the curve tangents. Yet, this tangent plane only defines the normal direction, not its orientation. We remove this sign ambiguity at the scale of a cycle by comparing normal orientations between successive nodes. Along a curve, we can compute a family of vectors by parallel-transporting the normal from one of its nodes [26]. These vectors are a good approximation of the normals of the underlying surface if the curve lies on this surface without significant geodesic torsion, which is the case for curvature lines that form a large part of designer-drawn curves [29, 39, 48]. Based on this observation, parallel-transporting the normal \vec{N}_A from node A to node B gives a vector $\vec{N}_{A||B}$ that should closely match the direction of normal \vec{N}_B . If the two vectors point in opposite directions, we flip \vec{N}_B before proceeding with the next node along the cycle, as illustrated in Fig. 6.

We apply this cycle detection on both sides of each new curve segment, taking care of removing any existing cycle when a curve is drawn across it. We also run the cycle detection on every segment that intersects user-deleted curves to update the surface after such edits.

While simple and efficient, the above algorithm is limited to smooth surfaces for which the tangent plane is well-defined at each curve intersection. If a node lies on a sharp surface feature, such as the corner of a cube, then several surface normals exist at that node (Fig. 7). We detect such cases by checking the residual of the tangent plane fitting, given by the maximum value among the dot products of the plane normal with the incident curve tangents. We consider that a node is on a sharp feature if this residual is above $\epsilon_{\text{sharp}} = 0.3$. On encountering such a node, we rely on the last well-defined normal along the cycle, which we transport to the node to sort its segments. We also take care of excluding the segments that do not lie close to the plane defined by this normal. In the rare case where the starting node of a cycle is itself sharp, we first resort to the normal of the best-fit plane to sort the segments incident to that node, and then for each successive pair of segments we look for a cycle with starting normal defined as the cross product between these two segments.

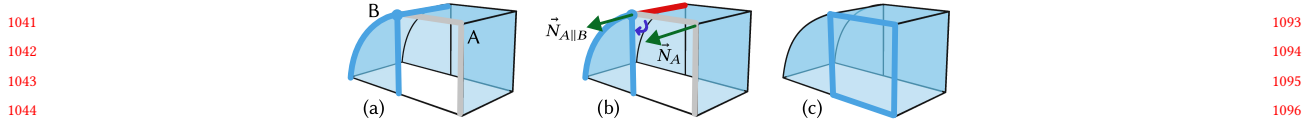


Fig. 7. Dealing with sharp surface features. The surface normal is ill-defined at node B , as one of the incident segments does not lie in the plane formed by the other ones (a). We exclude the segment that is not in the plane defined by the parallel-transported normal $\vec{N}_{A||B}$ (b, red) and select the next segment in clockwise order around $\vec{N}_{A||B}$ among the remaining options to form the cycle (c). In cases where the starting node A is also ill-defined, we compute the surface normal \vec{N}_A as the cross-product of two successive segments (b, gray) among the segments at A sorted according to the normal of the best-fit tangent plane.

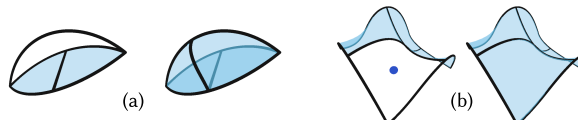


Fig. 8. The automatic cycle detection might fail. Adding strokes resolves the issue by creating additional intersections (a). It is also possible to manually add a patch by clicking (b).

Nevertheless, our automatic algorithm sometimes fails to detect cycles, especially on sparse curve networks as in Fig. 8a. Furthermore, our assumption that the curves exhibit little geodesic torsion does not always hold. While adding new curves to form a denser network often resolves these issues, we also allow users to explicitly trigger the creation of a surface patch by clicking near the center of the patch they envision (Fig. 8b). We then detect the closest stroke segment to the click and walk along the curve network by always selecting the segment that goes most towards the direction of the click. We also allow users to delete unwanted surface patches, for instance to create holes.

5.2 Surface geometry

Once a cycle is detected, we generate a triangle mesh over it with the method by Zou et al. [57], using their public implementation. We then refine the generated surface by applying isotropic re-meshing followed by curvature-flow smoothing [14, 32] to generate minimal (soap-film) surfaces. Both steps are performed using CGAL [52].

5.3 Sketching on surfaces

The surface patches generated by our method not only enhance the perception of the created shape, they can also serve the role of a canvas on which users can draw additional details. We consider that a stroke should lie on a surface patch if a) all of its control points are within a distance $r_{\text{proximity}}$ from that patch; and b) the curve does not split the cycle bounding the patch. When these criteria are fulfilled, we project all control points of the curve onto the surface patch so that the user stroke appears to stick to the object.

6 USER EXPERIENCE STUDY

We conducted a study to evaluate whether the user experience achieved with stroke neatening and surfacing is comparable to free-form sketching, making CASSIE a homogeneous solution bridging ideation sketching and concept modeling in AR/VR. A second goal of our study was to evaluate the effectiveness of our algorithms in neatening the user strokes and creating well-connected models. To this end, our study participants tried and evaluated three versions of the tool: a baseline *freehand* version which only contained mid-air sketching features, an *armature* version which

1145 implemented our curve neatening and structuring featureset, and a *patch* version which also included the automatic
 1146 and manual surfacing features, and the ability to draw on surface patches. We performed this study with expert and
 1147 novice users who are all familiar with VR interfaces in general.
 1148

1149 6.1 Participants

1151 We recruited 12 participants (2 female) aged 25–50 for the study. Six of the participants were professional artists or
 1152 designers, while the others had at least basic experience in CAD modelling or creating design sketches as part of their
 1153 jobs in graphics, HCI, or related fields and as hobbyists. All but two had used VR for over a year, and most (9/12) had
 1154 utilized VR for creative tasks, using Tilt Brush, Medium, Masterpiece VR, Blocks, AnimVR, or research prototypes.
 1155 Participants were paid approximately US \$22 for their time, converted to their currency of choice.
 1156

1158 6.2 Apparatus

1160 Owing to the restrictions on in-person user studies due to the COVID-19 pandemic, the study sessions were conducted
 1161 remotely, using participants' own VR setups. As a result, participants used a variety of VR devices, including Oculus
 1162 Rift and Rift S, HTC Vive, Vive Pro, and Vive Pro Eye. During the study session, an experimenter was available via
 1163 video-conferencing for answering participant questions.
 1164

1166 6.3 Procedure

1167 Participants first used the three systems to draw a computer mouse. These untimed sessions were utilized as tutorial
 1168 sessions, intended to let the participants familiarize themselves with the interface. Then, the participants used the three
 1169 systems in the same order as the tutorial for timed sessions, which were later utilized for qualitative and quantitative
 1170 analyses. For each system, participants were given 5 minutes to design a desk lamp followed by another 5 minutes
 1171 to create a running shoe. To reduce the influence of learning effects, the order of the systems was counterbalanced
 1172 between participants using a Latin square design. It is important to note that participants were not constrained to draw
 1173 the same shape with all the three systems. Instead, we asked them to work with the capabilities and constraints of each
 1174 system to design the optimal object.
 1175

1176 Each participant was sent a set of instructions a day before their study slot (see supplemental), informing them of
 1177 the nature of the research, the objects they were expected to draw, and the expected drawing style of a sparse curve
 1178 network. We hoped that this preparatory material helped participants think ahead and plan their designs in advance,
 1179 thus focusing on concept modeling in addition to pure ideation. However, participants were not required to do so.
 1180

1181 The study session started with participants signing an informed consent form, followed by them watching a detailed
 1182 instructions video (11 min, see supplemental material), and filling out a demographics questionnaire. After evaluating
 1183 each system, participants took a break and filled a short questionnaire for that system. Finally, participants filled a more
 1184 detailed questionnaire comparing the three systems.
 1185

1188 6.4 Results

1190 Fig. 9 shows the 3D sketches and models created by the six participants who declared to be professional artists. We
 1191 provide the creations of the six other participants as supplemental material.
 1192

1193 Most participants created shapes of similar complexity with all three systems (65 strokes on average for *freehand*, 44
 1194 for *armature*, 42 for *patch*, with no statistically significant difference between the three), although some participants
 1195 took advantage of the *freehand* system to achieve a more sketchy style with significant over-sketching (P5). Under
 1196

1197
 1198
 1199
 1200
 1201
 1202
 1203
 1204
 1205
 1206
 1207
 1208
 1209
 1210
 1211
 1212
 1213
 1214
 1215
 1216
 1217
 1218
 1219
 1220
 1221
 1222
 1223
 1224
 1225
 1226
 1227
 1228
 1229
 1230
 1231
 1232
 1233
 1234
 1235
 1236
 1237
 1238
 1239
 1240
 1241
 1242
 1243
 1244
 1245
 1246
 1247
 1248

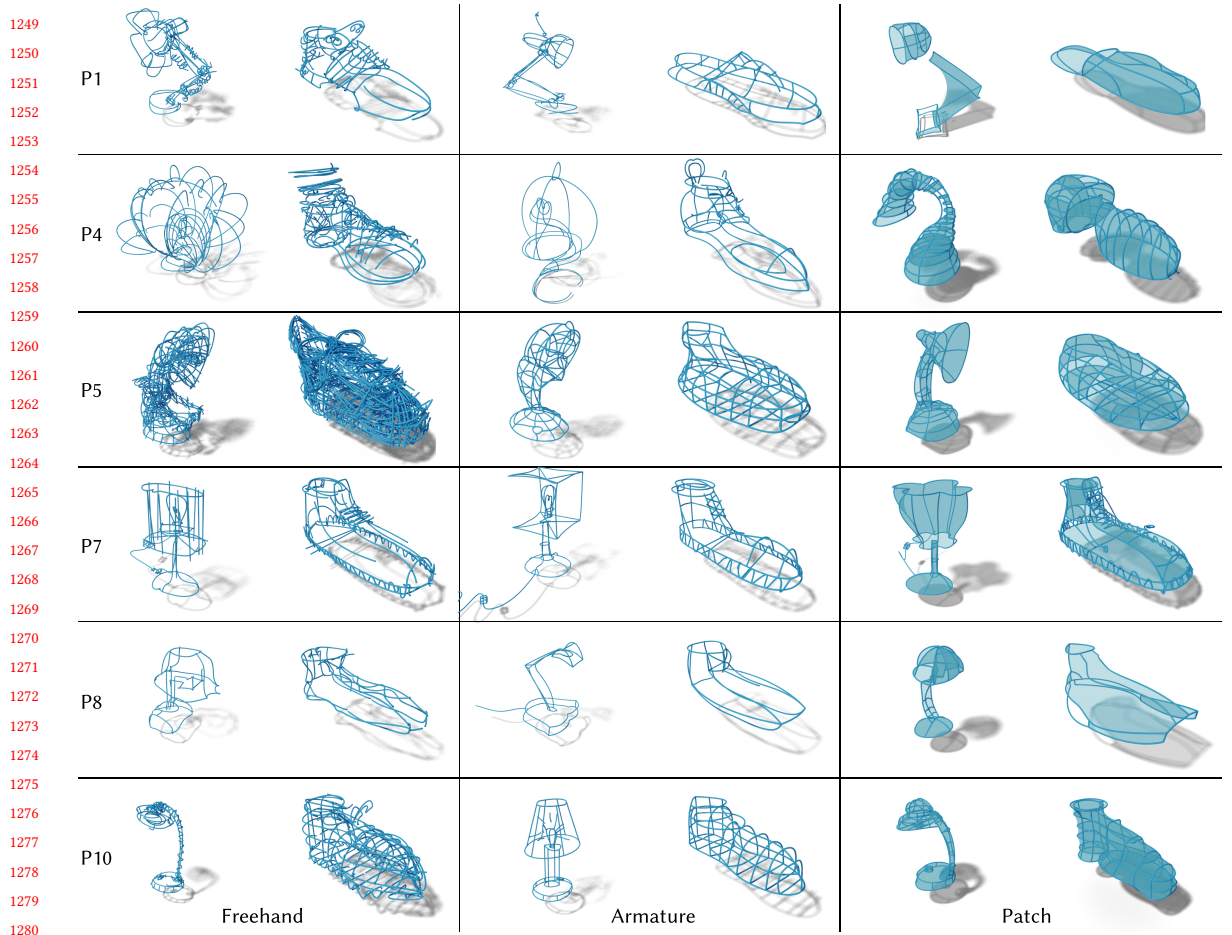


Fig. 9. Designs created by the six professional participants in the study using all three systems. We provide the results created by amateurs as supplemental material, although we didn't observe strong differences between the two groups.

close inspection, most *freehand* sketches exhibit over-shooting and gaps at stroke ends, which are mostly absent in the drawings created with the *armature* and *patch* systems. Finally, several of the models created with the *patch* system contain spurious holes in the 3D surface, which are either due to disconnected curves in the sketched network, or to failure of the automatic cycle detection algorithm.

Fig. 10 shows two drawings created in the *armature* system next to the raw strokes before snapping, which illustrates the approximate user inputs and the net effect of stroke neatening, structuring, and snapping.

We next discuss participants' feedback about their experience with the three systems, and then perform quantitative analysis of the curve networks they created.

6.4.1 User feedback. Users evaluated the degree of creative support provided by each system via the Creative Support Index (CSI) questionnaire [10]. We skipped the collaboration part of the questionnaire, as we did not build any collaborative tools in our systems. The summary results are shown in Table 1. The three systems fare almost evenly,

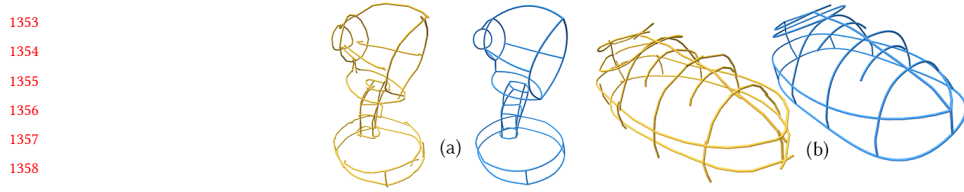


Fig. 10. Input strokes (yellow) and beautified result (blue) for sketches by P12 (a) and P9 (b). Notice how our beautification creates well-connected curve networks while deviating minimally from the original user strokes. Images rendered using Polyscope [49].

Table 1. Creative Support Index (CSI) [10] scores (out of 20) for each of the 3 systems (mean and standard deviation). Statistically significant differences are marked with asterisks (*). These scores put *armature* and *patch* on par with the *freehand* system, showing that the additional mental load imposed by these two systems did not cause a noticeable drop in users' creative potential.

	Freehand	Armature	Patch
Enjoyment	16.8 (2.7)	15.5 (2.4)	16.2 (2.7)
Exploration	15.0* (4.3)	13.1* (4.4)	13.5 (4.3)
Expressiveness	16.8 (2.9)	14.6 (3.2)	14.6 (3.6)
Immersion	16.6 (2.4)	15.5 (2.3)	15.2 (3.5)
Results Worth Effort	15.1 (3.5)	16.1 (1.9)	15.6 (3.0)
CSI	16.1	15.0	15.0

most differences being statistically insignificant ($p > .05$ on a repeated-measures ANOVA), except for *Exploration* where the *freehand* system outperforms the two others.

Participants commented that each system offered support for a slightly different portion of the *ideation-concept design continuum*: “Each has its own uses. Freehand is good for quickly sketching up an idea as you are not restricted by the system. Armature is good for refining a design...” (P11), “Armature seems [to be] a way to express volumes for more technical goals, but sketching [freehand] expresses an idea.” (P1) Some wanted to be able to quickly switch back-and-forth between the systems, a feature we implemented after the study: “[Armature] handles noise coming from the input motion and signal and creates a much nicer looking stroke. It would be nice to be able to turn off snapping however, to allow strokes to be drawn closer together.” (P3) In particular, automatic curve neatening reaches its limits on detailed sketches: “...predictive neatening was useful to help me quickly block out the initial shape, and snapping to form continuous lines was helpful since I was able to break up a complex stroke into smaller ones. But when the sketch became more complex and I had to draw finer/smaller strokes, it often “over-neatened” my strokes.” (P7)

Still, to compare the three systems, participants were asked to rate the value of the *armature* features compared to *freehand*, and the value of the *patch* system compared to *armature* on 5-point Likert scales (5 is highest). Most participants agreed that *armature* features added to the *freehand* system (6×5, 6×3, **median 4**) and the *patch* features were a valuable addition over *armature* (5×5, 4×4, 2×3, 1×2, **median 4**). Participants felt that the curve network *armatures* encouraged them to think more about the object’s use in downstream processes: “...with armature you can see the beautified sketch closer to a final draft.” (P8), “In the freehand method, I find I’m more inclined to do a messy sketch model rather than a more thought out one when using the armature system.” (P4)

The surface *patches* further bolstered this idea, motivating the creation of solid, usable, real-world shapes: “The patch system let [sic] you understand the geometry to create solid object necessary for many projects in an organic way. As

1457 for armature you can't see this right away taking an extra step in the process." (P8), "The patch system visually assisted
1458 my understanding of the model, [it] seemed to give me a better sense of its volume." (P9) Similarly, P2 commented that
1459 *patch* "allows users to define [a] surface without many lines which can clutter a design and possibly de-emphasise
1460 important features that need line definition [sic]."
1461

1462 However, the incentive to create well-connected curve networks in the *patch* system was also experienced as a
1463 constraint by some: "I found that using the patch system actually distracted me with trying to get the patching correct
1464 over the act of just sketching out what I was thinking about." (P4), "I felt that I had to change the way I worked to
1465 accommodate the system. For example, I would have to add more strokes to get the patches to show up, which meant that
1466 I deviate from my initial intent, or create a messier/busier looking drawing than I would have liked." (P7) Nevertheless,
1467 all the participants felt that they could derive value by incorporating the *armature* and *patch* functionalities in their
1468 typical workflow. For instance, P10 remarked that the systems were ideal for conceptualization: "Could be a great way
1469 to define rough shapes before bringing them into a desktop app to refine."
1470

1471 Lastly, while we did not imagine our tools being directly used for collaboration, P4 commented that they would use
1472 *armature* and *patch* "in collaboration environments where I would need to quickly express a 3D concept to colleagues."
1473

1474
1475
1476
1477 6.4.2 *Quantitative analysis*. Our goal when designing CASSIE was to support users in creating well-connected curve
1478 networks that can be surfaced for downstream applications. While visual comparison between *freehand* sketches and
1479 *armatures* show that the latter are much more connected, we hypothesize that the *patch* system provides additional
1480 incentive to create connected networks by rewarding participants when they do so. We evaluate this hypothesis by
1481 computing, for both *armature* and *patch* curve networks, the ratio of endpoint (dangling) nodes out of all nodes. We
1482 find out that the curve networks created with *patch* contain fewer endpoint nodes ($\mu = 9.8\%$, $\sigma = 6.8\%$) compared to
1483 *armature* ($\mu = 14.9\%$, $\sigma = 11.4\%$), meaning that they are better connected. The difference is statistically significant
1484 ($t = 2.50$, $p = .020$ on a paired t -test). The variance of this metric is also lower with the *patch* system, suggesting that
1485 more participants tended to sketch well-connected networks with *patch*.
1486

1487 While the *armature* and *patch* systems attempt to detect curve intersections automatically, they might sometimes
1488 miss intended intersections, or create unintended ones. When this is the case, users typically delete the stroke and
1489 redraw a new version that better reflects their goal. In contrast, users of the *freehand* system might correct for
1490 erroneous strokes simply by over-sketching duplicate strokes. We quantify these different strategies by counting the
1491 ratio of deleted strokes for each system: *freehand* ($\mu = 27.2\%$, $\sigma = 14.1\%$), *armature* ($\mu = 36.3\%$, $\sigma = 12.5\%$), *patch*
1492 ($\mu = 39.5\%$, $\sigma = 13.3\%$). A repeated-measures ANOVA reveals that users deleted significantly less strokes in the *freehand*
1493 system ($F_{2,22} = 6.93$, $p = .005$).
1494

1495 7 RESULTS AND APPLICATIONS

1500 Fig. 11 provides a gallery of models created with CASSIE by several trained users, including a professional study
1501 participant (P1) and 3 different authors. The sketches cover diverse application domains such as product design (a,b,e,g),
1502 architecture (c,d), and character design (f). Note how VR sketching facilitates design in context, as illustrated with the
1503 VR headsets drawn using a 3D head as an underlay to achieve accurate proportions and contacts. Most sketches were
1504 done in short sessions of 5–20 minutes, while the 1:1 scale car design (3.2m in length) took an hour and 40 minutes.
1505

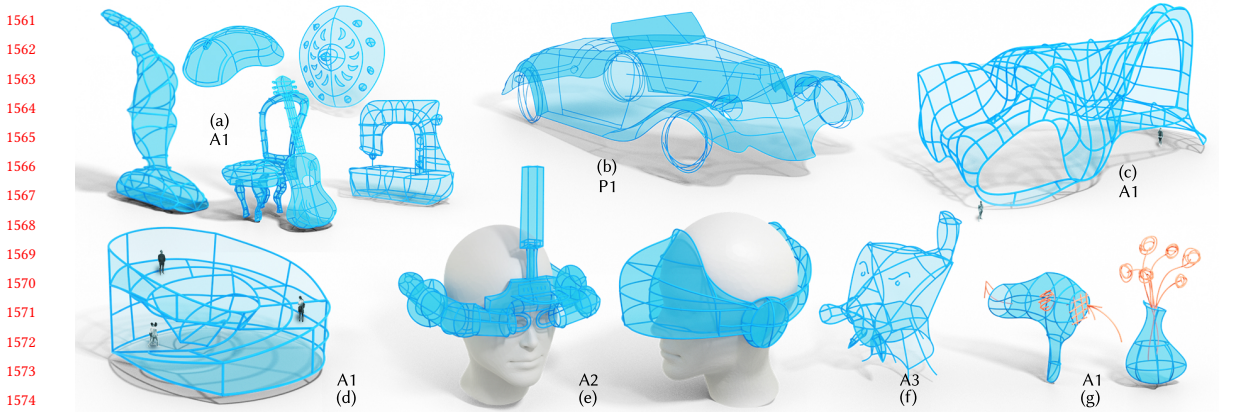


Fig. 11. A gallery of 3D sketches created with CASSIE, labelled with the creator (A: author, P: participant). While most designs made use of the *armature* and *patch* features, some also included freehand strokes (orange) to suggest less definite parts (h).

7.1 Comparisons

We compared our system to GravitySketch [24], a commercial software that allows the creation of 3D curves and surfaces in VR. A major difference between this system and ours is that GravitySketch provides completely independent facilities for curve and surface creation that are switched between using a modal interface. As a result, users typically first lay down the salient feature curves of the model before draping these curves with surface patches. Since the curves are drawn without explicit connectivity, users need to explicitly define every single surface patch to be created, as illustrated in Fig. 12 that shows a sequence of modeling steps extracted from an online tutorial (https://youtu.be/ymCe5C_llF4). In contrast, users of CASSIE can quickly create a similar model by seamlessly drawing the feature curves over the inferred surface patches. P1 particularly liked how CASSIE’s fluid interface contrasted with their prior experience with GravitySketch, remarking verbally: “In [desktop-based] CAD tools one is more forgiving of an engineering style workflow but in VR the mind-set is fluidity.”

Another comparison can be drawn to sketch-based modeling tools that *lift* 2D sketches into 3D. While CASSIE adopts a fluid, natural interface, such tools typically require designers to either follow a strict creation style [47] or provide additional manual annotations [55]. Moreover, layered or geometrically complex 3D objects—such as the hat (Fig. 1c), buildings (Fig. 11c-d), or HMDs (Fig. 11e)—that do not have a single descriptive 2D viewpoint [16] can be extremely cumbersome or impossible to design using purely 2D sketch-based modeling tools.

7.2 Downstream processing

3D models created in CASSIE are readily usable in downstream software, as illustrated in the following proofs-of-concept.

Rapid prototyping. While our system generates each surface patch independently, we can use existing remeshing tools [11, 28] to merge them into a single, manifold surface suitable for 3D printing. Fig. 13a–b shows two such physical prototypes created with CASSIE.

Engineering. Our surfaced models also offer a bridge between conceptual design and engineering, as illustrated in Fig. 13c where we used the method by Arora et al. [4] to generate a volumetric truss structure inside the object, aligned with its primary directions of stress.

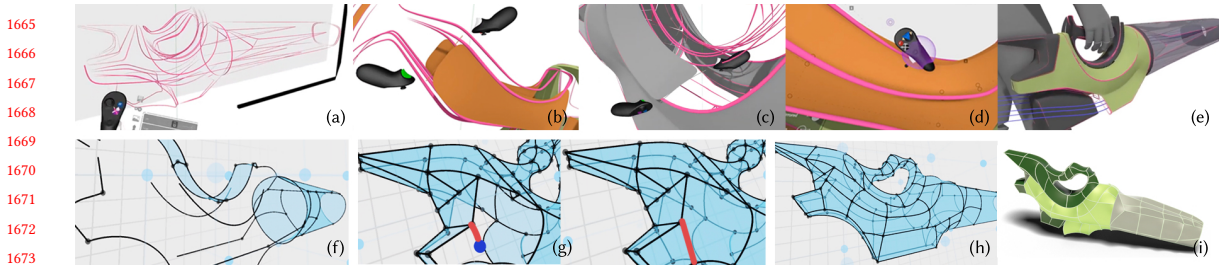


Fig. 12. Comparing design workflows in GravitySketch [24] (top) and CASSIE (bottom). In GravitySketch, the user starts with a loose sketch composed of strokes with no explicit connectivity (a). Adding surfaces comes at a later stage, either by bridging nearby curves (b) or by roughly aligning the surface to the strokes (c). The user can then refine the surfaces via control points. With CASSIE, the user simultaneously sketches well-connected curve networks (f) and surfaces automatically appear as a cycle is closed (g) by a new stroke (red). The user can refine the surfaces by adding strokes that directly control the shape of the surface (h). The final result is a leaf blower (e,i), which we colored and rendered in Blender. A video version of this comparison is provided in the supplements.

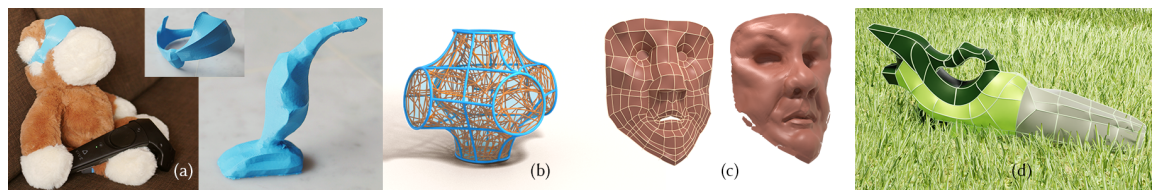


Fig. 13. Applications: (a) 3D printed HMD from Fig. 11f and vacuum cleaner from Fig. 11a, (b) structural analysis and truss generation using Arora et al. [4], (c) detailed face model sculpted by P5 by sketching in CASSIE (left) and then refining patches in ZBrush [42] (right), (d) colored and shaded render to use as communication material.

Surface sculpting. Fig. 13d illustrates a sequential workflow where CASSIE is used to quickly design the main features of an object, before being refined in a commercial sculpting application [42].

Concept presentation. Finally, 3D objects designed with CASSIE can be colored and shaded for presentation (Fig. 13d).

8 CONCLUSION AND FUTURE WORK

Ideation and concept modeling are the foundation of 3D design. In current practice, 2D sketches dominate ideation, and disparate CAD-like tools produce 3D concept models. Our system CASSIE showcases the ability of AR/VR to effectively support both ideation and concept modeling in a shared immersive space. CASSIE combines the fluidity of freehand sketching with geometric and aesthetic constraints of 3D modeling, to predictively neatens, structure, and surface user strokes into 3D models of sufficient quality for downstream applications. Importantly, our study reveals that such progressive structuring and surfacing is not detrimental to user agency, significantly helps users perceive an evolving 3D shape, and acts as an incentive to draw well-connected 3D concept models.

Limitations: While automatic neatening greatly eases the creation of connected curve networks, our current implementation based on a single proximity threshold was judged too intrusive by some participants. Several strategies could be explored to provide finer control on snapping, such as adapting the threshold to stroke speed or pressure, or learning a user-specific threshold by analyzing a few annotated freehand drawings of that user. Surface generation could also be improved, for instance by better reproducing the curvature depicted by the armature [39]. In order to bootstrap these efforts, we will openly release the interaction data from the 72 sketches in our study as well as the 16

1769 other sketches depicted in the paper, including raw user strokes as well as the neatened curves. We will also release the
1770 CASSIE source code for academic research.

1771 *Future Work:* While our current prototype allows users to switch between creative exploration and more precise
1772 modeling simply by enabling neatening and surfacing, we see several avenues to achieve a continuum between these
1773 two forms of sketching. On the one hand, freehand strokes could be used as underlays to trace more definite armatures,
1774 and as extra guidance in our optimization to best position the neatened curves and surface patches. On the other hand,
1775 sparse armatures could be used as structured spatial deformers to warp denser freehand strokes, allowing designers to
1776 explore design variations while retaining the original look of their ideation sketches. The AR/VR setting could also be
1777 leveraged for sketching in situ, as suggested with the headsets sketched over a head in Fig. 11. In this usage scenario,
1778 the contextual 3D models could be used as extra cues for stroke beautification and surface generation.
1779

1780 We believe that mid-air drawing in immersive environments has the potential to significantly disrupt the interactive
1781 3D design process, and CASSIE is a positive step in that direction.
1782

REFERENCES

- 1786 [1] Fatemeh Abbasinejad, Pushkar Joshi, and Nina Amenta. 2011. Surface patches from unorganized space curves. *Computer Graphics Forum* 30, 5 (2011), 1379–1387. <https://doi.org/10.1111/j.1467-8659.2011.02012.x>
- 1787 [2] Rahul Arora, Ishan Darolia, Vinay P Namboodiri, Karan Singh, and Adrien Bousseau. 2017. Sketchsoup: Exploratory Ideation using Design Sketches. *Computer Graphics Forum* 36, 8 (2017), 302–312.
- 1788 [3] Rahul Arora, Rubaiat Habib Kazi, Tovi Grossman, George Fitzmaurice, and Karan Singh. 2018. SymbiosisSketch: Combining 2d & 3d sketching for designing detailed 3d objects in situ. In *Proceedings of the 2018 CHI Conference on Human Factors in Computing Systems*. ACM, New York, NY, USA, 1–15.
- 1789 [4] Rahul Arora, Alec Jacobson, Timothy R. Langlois, Yijiang Huang, Caitlin Mueller, Wojciech Matusik, Ariel Shamir, Karan Singh, and David I.W. Levin. 2019. Volumetric Michell Trusses for Parametric Design & Fabrication. In *Proceedings of the 3rd ACM Symposium on Computation Fabrication* (Pittsburgh, PA, USA) (SCF '19). ACM, New York, NY, USA, 13.
- 1790 [5] Rahul Arora, Rubaiat Habib Kazi, Fraser Anderson, Tovi Grossman, Karan Singh, and George W Fitzmaurice. 2017. Experimental Evaluation of Sketching on Surfaces in VR.. In *CHI*, Vol. 17. ACM, New York, NY, USA, 5643–5654.
- 1791 [6] Robert McNeel & Associates. 2018. Rhinoceros 3D. <https://www.rhino3d.com/>.
- 1792 [7] Seok-Hyung Bae, Ravin Balakrishnan, and Karan Singh. 2008. ILoveSketch: as-natural-as-possible sketching system for creating 3d curve models. In *Proceedings of the 21st annual ACM symposium on User interface software and technology*. ACM, New York, NY, USA, 151–160.
- 1793 [8] Ravin Balakrishnan, George Fitzmaurice, Gordon Kurtenbach, and William Buxton. 1999. Digital tape drawing. In *Proceedings of the 12th annual ACM symposium on User interface software and technology*. ACM, New York, NY, USA, 161–169.
- 1794 [9] Mikhail Bessmeltsev, Caoyu Wang, Alla Sheffer, and Karan Singh. 2012. Design-driven quadrangulation of closed 3D curves. *ACM Transactions on Graphics (TOG)* 31, 6 (2012), 1–11.
- 1795 [10] Erin Cherry and Celine Latulipe. 2014. Quantifying the Creativity Support of Digital Tools through the Creativity Support Index. *ACM Trans. Comput.-Hum. Interact.* 21, 4, Article 21 (June 2014), 25 pages. <https://doi.org/10.1145/2617588>
- 1796 [11] Paolo Cignoni, Massimiliano Corsini, and Guido Ranzuglia. 2008. MeshLab: an Open-Source 3D Mesh Processing System. *ERCIM News* 73 (2008), 47–48. <http://dblp.uni-trier.de/db/journals/ercim/ercim2008.html#CignoniCR08>
- 1797 [12] Chris De Paoli and Karan Singh. 2015. SecondSkin: sketch-based construction of layered 3D models. *ACM Transactions on Graphics (TOG)* 34, 4 (2015), 1–10.
- 1798 [13] Michael F Deering. 1995. HoloSketch: a virtual reality sketching/animation tool. *ACM Transactions on Computer-Human Interaction (TOCHI)* 2, 3 (1995), 220–238.
- 1799 [14] Mathieu Desbrun, Mark Meyer, Peter Schröder, and Alan H Barr. 1999. Implicit fairing of irregular meshes using diffusion and curvature flow. In *Proceedings of the 26th annual conference on Computer graphics and interactive techniques*. ACM, New York, NY, USA, 317–324.
- 1800 [15] Julie Dorsey, Songhua Xu, Gabe Smedresman, Holly Rushmeier, and Leonard McMillan. 2007. The Mental Canvas: A Tool for Conceptual Architectural Design and Analysis. In *Proc. IEEE Pacific Conference on Computer Graphics and Applications*. IEEE, New York, NY, USA, 201–210.
- 1801 [16] K Eissen and R Steur. 2009. *Sketching: Drawing techniques for product designers* (11 ed.). BIS Publishers, AMsterdam, The Netherlands.
- 1802 [17] Facebook. 2015. Oculus Medium. <https://www.oculus.com/medium/>.
- 1803 [18] Facebook. 2016. Oculus Quill. <https://www.oculus.com/experiences/rift/1118609381580656/>.
- 1804 [19] Michele Fiorentino, Raffaele de Amicis, Giuseppe Monno, and Andre Stork. 2002. Spacedesign: A mixed reality workspace for aesthetic industrial design. In *Proceedings. International Symposium on Mixed and Augmented Reality*. IEEE, New York, NY, USA, 86–318. <https://doi.org/10.1109/ISMAR.2002.1115077>

1821
1822
1823
1824
1825
1826
1827
1828
1829
1830
1831
1832
1833
1834
1835
1836
1837
1838
1839
1840
1841
1842
1843
1844
1845
1846
1847
1848
1849
1850
1851
1852
1853
1854
1855
1856
1857
1858
1859
1860
1861
1862
1863
1864
1865
1866
1867
1868
1869
1870
1871
1872

- 1873 [20] Jakub Fišer, Paul Asente, and Daniel Sýkora. 2015. ShipShape: a drawing beautification assistant. In *Proceedings of the workshop on Sketch-Based Interfaces and Modeling*. Eurographics Association, Geneve, Switzerland, 49–57. 1925
- 1874 [21] Google. 2016. Tilt Brush. <https://www.tiltbrush.com>. 1926
- 1875 [22] Google. 2017. Google Blocks. <https://arvr.google.com/blocks/>. 1927
- 1876 [23] Giorgio Gori, Alla Sheffer, Nicholas Vining, Enrique Rosales, Nathan Carr, and Tao Ju. 2017. Flowrep: Descriptive curve networks for free-form design shapes. *ACM Transactions on Graphics (TOG)* 36, 4 (2017), 1–14. 1928
- 1877 [24] GravitySketch. 2017. Gravity Sketch. <https://www.gravitysketch.com/>. 1929
- 1878 [25] Tovi Grossman, Ravin Balakrishnan, and Karan Singh. 2003. An Interface for Creating and Manipulating Curves Using a High Degree-of-Freedom Curve Input Device. In *Proc. of the ACM SIGCHI Conference on Human Factors in Computing Systems*. ACM, New York, NY, USA, 185–192. 1930
- 1879 [26] Andrew J Hanson and Hui Ma. 1995. Parallel transport approach to curve framing. *Indiana University, Techreports-TR425* 11 (1995), 3–7. 1931
- 1880 [27] Laura M. Herman and Stefanie Hutka. 2019. Virtual Artistry: Virtual Reality Translations of Two-Dimensional Creativity. In *Proceedings of the 2019 on Creativity and Cognition* (San Diego, CA, USA) (C&C '19). Association for Computing Machinery, New York, NY, USA, 612–618. 1932
- 1881 [28] Yixin Hu, Qingnan Zhou, Xifeng Gao, Alec Jacobson, Denis Zorin, and Daniele Panozzo. 2018. Tetrahedral Meshing in the Wild. *ACM Trans. Graph.* 37, 4, Article 60 (July 2018), 14 pages. <https://doi.org/10.1145/3197517.3201353> 1933
- 1882 [29] Emmanuel Iarussi, David Bommes, and Adrien Bousseau. 2015. BendFields: Regularized Curvature Fields from Rough Concept Sketches. *ACM Trans. Graph.* 34, 3, Article 24 (May 2015), 16 pages. <https://doi.org/10.1145/2710026> 1934
- 1883 [30] Takeo Igarashi, Satoshi Matsuoka, Sachiko Kawachiya, and Hidehiko Tanaka. 2007. Interactive beautification: a technique for rapid geometric design. In *ACM SIGGRAPH 2007 courses*. ACM, New York, NY, USA, 18–es. 1935
- 1884 [31] Bret Jackson and Daniel F Keefe. 2016. Lift-off: Using reference imagery and freehand sketching to create 3d models in VR. *IEEE transactions on visualization and computer graphics* 22, 4 (2016), 1442–1451. 1936
- 1885 [32] Michael Kazhdan, Jake Solomon, and Mirela Ben-Chen. 2012. Can mean-curvature flow be modified to be non-singular? *Computer Graphics Forum* 31, 5 (2012), 1745–1754. 1937
- 1886 [33] Daniel Keefe, Robert Zeleznik, and David Laidlaw. 2007. Drawing on air: Input techniques for controlled 3D line illustration. *IEEE Transactions on Visualization and Computer Graphics* 13, 5 (2007), 1067–1081. 1938
- 1887 [34] Yongkwan Kim, Sang-Gyun An, Joon Hyub Lee, and Seok-Hyung Bae. 2018. Agile 3D sketching with air scaffolding. In *Proceedings of the 2018 CHI Conference on Human Factors in Computing Systems*. ACM, New York, NY, USA, 1–12. 1939
- 1888 [35] Chenxi Liu, Enrique Rosales, and Alla Sheffer. 2018. Strokeaggregator: Consolidating raw sketches into artist-intended curve drawings. *ACM Transactions on Graphics (TOG)* 37, 4 (2018), 1–15. 1940
- 1889 [36] Mayra D Barrera Machuca, Paul Asente, Wolfgang Stuerzlinger, Jingwan Lu, and Byungmoon Kim. 2018. Multiplanes: Assisted freehand VR Sketching. In *Proceedings of the Symposium on Spatial User Interaction*. ACM, New York, NY, USA, 36–47. 1941
- 1890 [37] Mayra Donaji Barrera Machuca, Wolfgang Stuerzlinger, and Paul Asente. 2019. The Effect of Spatial Ability on Immersive 3D Drawing. In *Proceedings of the ACM Conference on Creativity & Cognition (C&C'19)*. ACM, New York, NY, USA, 173–186. 1942
- 1891 [38] Patrick Paczkowski, Min H. Kim, Yann Morvan, Julie Dorsey, Holly Rushmeier, and Carol O'Sullivan. 2011. Insitu: Sketching Architectural Designs in Context. *ACM Trans. Graph.* 30, 6 (Dec. 2011), 1–10. <https://doi.org/10.1145/2070781.2024216> 1943
- 1892 [39] Hao Pan, Yang Liu, Alla Sheffer, Nicholas Vining, Chang-Jian Li, and Wenping Wang. 2015. Flow aligned surfacing of curve networks. *ACM Transactions on Graphics (TOG)* 34, 4 (2015), 1–10. 1944
- 1893 [40] Theo Pavlidis and Christopher J Van Wyk. 1985. An automatic beautifier for drawings and illustrations. *ACM SIGGRAPH Computer Graphics* 19, 3 (1985), 225–234. 1945
- 1894 [41] A. Pipes. 2007. *Drawing for Designers*. Laurence King Publishing, London, UK. <https://books.google.co.nz/books?id=phgfAQAAIAAJ> 1946
- 1895 [42] Pixologic. 2016. ZBrush. <http://pixologic.com/features/about-zbrush.php>. 1947
- 1896 [43] Enrique Rosales, Jafet Rodriguez, and Alla Sheffer. 2019. SurfaceBrush: From Virtual Reality Drawings to Manifold Surfaces. *ACM Transaction on Graphics* 38, 4, Article 96 (2019), 15 pages. <https://doi.org/10.1145/3306346.3322970> 1948
- 1897 [44] Emanuel Sachs, Andrew Roberts, and David Stoops. 1991. 3-Draw: A tool for designing 3D shapes. *IEEE Computer Graphics and Applications* 11, 6 (1991), 18–26. 1949
- 1898 [45] Bardia Sadri and Karan Singh. 2014. Flow-Complex-Based Shape Reconstruction from 3D Curves. *ACM Transactions on Graphics* 33, 2, Article 20 (2014), 15 pages. 1950
- 1899 [46] Steven Schkolne, Michael Pruett, and Peter Schröder. 2001. Surface drawing: creating organic 3D shapes with the hand and tangible tools. In *Proceedings of the SIGCHI conference on Human factors in computing systems*. ACM, New York, NY, USA, 261–268. 1951
- 1900 [47] Ryan Schmidt, Azam Khan, Karan Singh, and Gord Kurtenbach. 2009. Analytic drawing of 3D scaffolds. *ACM transactions on graphics (TOG)* 28, 5 (2009), 1–10. 1952
- 1901 [48] Cloud Shao, Adrien Bousseau, Alla Sheffer, and Karan Singh. 2012. CrossShade: shading concept sketches using cross-section curves. *ACM Transactions on Graphics (TOG)* 31, 4, Article 45 (2012), 11 pages. 1953
- 1902 [49] Nicholas Sharp et al. 2019. Polyscope. www.polyscope.run. 1954
- 1903 [50] Tibor Stanko, Stefanie Hahmann, Georges-Pierre Bonneau, and Nathalie Saguin-Sprynski. 2016. Smooth interpolation of curve networks with surface normals. In *EG 2016 - Short Papers*. The Eurographics Association, Geneve, Switzerland, 21–24. 1955
- 1904 [51] Nicholas Sharp et al. 2019. Polyscope. www.polyscope.run. 1956
- 1905 [52] Tibor Stanko, Stefanie Hahmann, Georges-Pierre Bonneau, and Nathalie Saguin-Sprynski. 2016. Smooth interpolation of curve networks with surface normals. In *EG 2016 - Short Papers*. The Eurographics Association, Geneve, Switzerland, 21–24. 1957
- 1906 [53] Tibor Stanko, Stefanie Hahmann, Georges-Pierre Bonneau, and Nathalie Saguin-Sprynski. 2016. Smooth interpolation of curve networks with surface normals. In *EG 2016 - Short Papers*. The Eurographics Association, Geneve, Switzerland, 21–24. 1958
- 1907 [54] Tibor Stanko, Stefanie Hahmann, Georges-Pierre Bonneau, and Nathalie Saguin-Sprynski. 2016. Smooth interpolation of curve networks with surface normals. In *EG 2016 - Short Papers*. The Eurographics Association, Geneve, Switzerland, 21–24. 1959
- 1908 [55] Tibor Stanko, Stefanie Hahmann, Georges-Pierre Bonneau, and Nathalie Saguin-Sprynski. 2016. Smooth interpolation of curve networks with surface normals. In *EG 2016 - Short Papers*. The Eurographics Association, Geneve, Switzerland, 21–24. 1960
- 1909 [56] Tibor Stanko, Stefanie Hahmann, Georges-Pierre Bonneau, and Nathalie Saguin-Sprynski. 2016. Smooth interpolation of curve networks with surface normals. In *EG 2016 - Short Papers*. The Eurographics Association, Geneve, Switzerland, 21–24. 1961
- 1910 [57] Tibor Stanko, Stefanie Hahmann, Georges-Pierre Bonneau, and Nathalie Saguin-Sprynski. 2016. Smooth interpolation of curve networks with surface normals. In *EG 2016 - Short Papers*. The Eurographics Association, Geneve, Switzerland, 21–24. 1962
- 1911 [58] Tibor Stanko, Stefanie Hahmann, Georges-Pierre Bonneau, and Nathalie Saguin-Sprynski. 2016. Smooth interpolation of curve networks with surface normals. In *EG 2016 - Short Papers*. The Eurographics Association, Geneve, Switzerland, 21–24. 1963
- 1912 [59] Tibor Stanko, Stefanie Hahmann, Georges-Pierre Bonneau, and Nathalie Saguin-Sprynski. 2016. Smooth interpolation of curve networks with surface normals. In *EG 2016 - Short Papers*. The Eurographics Association, Geneve, Switzerland, 21–24. 1964
- 1913 [60] Tibor Stanko, Stefanie Hahmann, Georges-Pierre Bonneau, and Nathalie Saguin-Sprynski. 2016. Smooth interpolation of curve networks with surface normals. In *EG 2016 - Short Papers*. The Eurographics Association, Geneve, Switzerland, 21–24. 1965
- 1914 [61] Tibor Stanko, Stefanie Hahmann, Georges-Pierre Bonneau, and Nathalie Saguin-Sprynski. 2016. Smooth interpolation of curve networks with surface normals. In *EG 2016 - Short Papers*. The Eurographics Association, Geneve, Switzerland, 21–24. 1966
- 1915 [62] Tibor Stanko, Stefanie Hahmann, Georges-Pierre Bonneau, and Nathalie Saguin-Sprynski. 2016. Smooth interpolation of curve networks with surface normals. In *EG 2016 - Short Papers*. The Eurographics Association, Geneve, Switzerland, 21–24. 1967
- 1916 [63] Tibor Stanko, Stefanie Hahmann, Georges-Pierre Bonneau, and Nathalie Saguin-Sprynski. 2016. Smooth interpolation of curve networks with surface normals. In *EG 2016 - Short Papers*. The Eurographics Association, Geneve, Switzerland, 21–24. 1968
- 1917 [64] Tibor Stanko, Stefanie Hahmann, Georges-Pierre Bonneau, and Nathalie Saguin-Sprynski. 2016. Smooth interpolation of curve networks with surface normals. In *EG 2016 - Short Papers*. The Eurographics Association, Geneve, Switzerland, 21–24. 1969
- 1918 [65] Tibor Stanko, Stefanie Hahmann, Georges-Pierre Bonneau, and Nathalie Saguin-Sprynski. 2016. Smooth interpolation of curve networks with surface normals. In *EG 2016 - Short Papers*. The Eurographics Association, Geneve, Switzerland, 21–24. 1970
- 1919 [66] Tibor Stanko, Stefanie Hahmann, Georges-Pierre Bonneau, and Nathalie Saguin-Sprynski. 2016. Smooth interpolation of curve networks with surface normals. In *EG 2016 - Short Papers*. The Eurographics Association, Geneve, Switzerland, 21–24. 1971
- 1920 [67] Tibor Stanko, Stefanie Hahmann, Georges-Pierre Bonneau, and Nathalie Saguin-Sprynski. 2016. Smooth interpolation of curve networks with surface normals. In *EG 2016 - Short Papers*. The Eurographics Association, Geneve, Switzerland, 21–24. 1972
- 1921 [68] Tibor Stanko, Stefanie Hahmann, Georges-Pierre Bonneau, and Nathalie Saguin-Sprynski. 2016. Smooth interpolation of curve networks with surface normals. In *EG 2016 - Short Papers*. The Eurographics Association, Geneve, Switzerland, 21–24. 1973
- 1922 [69] Tibor Stanko, Stefanie Hahmann, Georges-Pierre Bonneau, and Nathalie Saguin-Sprynski. 2016. Smooth interpolation of curve networks with surface normals. In *EG 2016 - Short Papers*. The Eurographics Association, Geneve, Switzerland, 21–24. 1974
- 1923 [70] Tibor Stanko, Stefanie Hahmann, Georges-Pierre Bonneau, and Nathalie Saguin-Sprynski. 2016. Smooth interpolation of curve networks with surface normals. In *EG 2016 - Short Papers*. The Eurographics Association, Geneve, Switzerland, 21–24. 1975
- 1924 [71] Tibor Stanko, Stefanie Hahmann, Georges-Pierre Bonneau, and Nathalie Saguin-Sprynski. 2016. Smooth interpolation of curve networks with surface normals. In *EG 2016 - Short Papers*. The Eurographics Association, Geneve, Switzerland, 21–24. 1976

- 1977 [51] Kenshi Takayama, Daniele Panozzo, Alexander Sorkine-Hornung, and Olga Sorkine-Hornung. 2013. Sketch-Based Generation and Editing of Quad
1978 Meshes. *ACM Transactions on Graphics (proceedings of ACM SIGGRAPH)* 32, 4 (2013), 97:1–97:8. 2029
1979 [52] The CGAL Project. 2020. *CGAL User and Reference Manual* (5.0.2 ed.). CGAL Editorial Board. <https://doc.cgal.org/5.0.2/Manual/packages.html> 2030
1980 [53] Floor Verhoeven and Olga Sorkine-Hornung. 2019. RodMesh: Two-handed 3D Surface Modeling in Virtual Reality. In *Proceedings of the Symposium*
1981 *on Vision, Modeling and Visualization (VMV)*. The Eurographics Association, Geneve, Switzerland, 10. 2032
1982 [54] Gerold Wesche and Hans-Peter Seidel. 2001. FreeDrawer: a free-form sketching system on the responsive workbench. In *Proceedings of the ACM*
1983 *symposium on Virtual reality software and technology*. ACM, New York, NY, USA, 167–174. 2033
1984 [55] Baoxuan Xu, William Chang, Alla Sheffer, Adrien Bousseau, James McCrae, and Karan Singh. 2014. True2Form: 3D curve networks from 2D sketches
1985 via selective regularization. *ACM Transactions on Graphics* 33, 4, Article 131 (2014), 13 pages. 2034
1986 [56] Yixin Zhuang, Ming Zou, Nathan Carr, and Tao Ju. 2013. A general and efficient method for finding cycles in 3D curve networks. *ACM Transactions*
1987 *on Graphics (TOG)* 32, 6 (2013), 1–10. 2035
1988 [57] Ming Zou, Tao Ju, and Nathan Carr. 2013. An algorithm for triangulating multiple 3D polygons. *Computer Graphics Forum* 32, 5 (2013), 157–166. 2036
1989 2037
1990 2038
1991 2039
1992 2040
1993 2041
1994 2042
1995 2043
1996 2044
1997 2045
1998 2046
1999 2047
2000 2048
2001 2049
2002 2050
2003 2051
2004 2052
2005 2053
2006 2054
2007 2055
2008 2056
2009 2057
2010 2058
2011 2059
2012 2060
2013 2061
2014 2062
2015 2063
2016 2064
2017 2065
2018 2066
2019 2067
2020 2068
2021 2069
2022 2070
2023 2071
2024 2072
2025 2073
2026 2074
2027 2075
2028 2076
2029 2077
2030 2078
2031 2079
2032 2080